

COMPUTATIONAL ESTIMATES OF STRESS INTENSITY FACTOR FOR CRACKS IN PLATES AND SHELLS USING A BIE METHOD

M. R. ETEMAD and C. E. TURNER*

Results generated using a BIE program to find LEFM shape factors for semi-elliptical surface cracks in several plate and shell cases are described. Data for nine wide plate cases with $a/c=0.3$ and 0.4 and $a/t=0.5, 0.4$ and 0.2 , subjected to remote uniform tensile loading are given and compared with those in the literature. Present results were found to be within the scatter of published data though 5-18% lower than the well known data of Newman & Raju. Initial results for three cracks in the circumference of cylinders subject to tension, with $a/c=0.14$, $a/t=0.6$, $R/t=29$ and $a/c=0.6$, $a/t=0.5$ and 0.6 , $R/t=11$, subjected to tension are found to be in good agreement with those of Newman & Raju. One case with local wall bending is also given.

INTRODUCTION

The usefulness of LEFM in defect assessment of engineering components and structures is greatly enhanced in practice if the behaviour of three-dimensional, 3D, crack problems can be predicted. This type of analysis is not always possible and use is made of simple models involving two dimensional, 2D, idealisations of these problems. Earlier references [1-7] have recently been complemented by a study of cracks in otherwise axisymmetric (quasi-2D) bodies, Kumar et al [8]. Their results agree with those of [5] to within 4% and of [2] to within 10%. A comparison of full 3D, 2D and quasi-2D results has shown the 3D results generally to be lower, emphasising the benefit of a full 3D analysis. A detailed comparative analysis of shape factor data for semi-elliptical surface cracks in both plate and shell geometries from sixteen sources, e.g. Refs.1 to 4, revealed considerable disagreement.

The boundary integral element, BIE, method is often cited as offering a solution procedure more convenient than the 3D finite element, FE, method. Its application to plates and shells is less favourable because of the need to maintain reasonable aspect ratios for the elements. Nevertheless, the present work uses a BIE analysis and is restricted to 160 elements as part of a study of whether a sub-structure approach to cracks in tubular joints as found in offshore structures is worth pursuing.

1. SURFACE CRACKS IN PLATES

For surface cracks the magnitude of K varies along the crack front. Only mode 1

*Mechanical Engineering Department, Imperial College, London SW7 2BX

(tensile opening) is considered here. These cracks are usually approximated by a semi-elliptical form, surface length, $2c$, penetration, a , with the position along the crack front defined by the angle ϕ , zero at the free surface. K is written

$$Y = (F\sqrt{\pi}) / Q \text{ where } \sqrt{Q} = \int_0^{\pi/2} (\cos^2 \phi + (a/c)^2 \sin^2 \phi)^{1/2} d\phi \text{ in } K = Y\sigma\sqrt{a}$$

The Q factor for an ellipse is a complete elliptical integral of the second type which can be approximated for $a/c < 1$

$$Q = [1 + 1.464(a/c)^{1.65}]^{1/2}$$

For $a/c > 1$ the same approximation is valid but with c/a replacing a/c . Extensive results by Newman and Raju using 3D FE methods, were reported [1] for a wide range of crack and plate geometries, including corner cracks and surface cracks at holes, with various crack depth to thickness ratios, a/t , and crack ellipticities, a/c . Empirical equations for F were given in [1] to fit surface crack data from [1i] and differences of up to 5% are referred to. For $a/c < 1$ or $a/t < 1$

$$F = [M1 + M2(a/t)^2 + M3(a/t)^4] g f k$$

$$M1 = 1.13 - 0.09(a/c) \text{ and } M2 = 0.54 + [0.89 / (0.2 + (a/c))]$$

$$M3 = 0.5 - [1 / (0.65 + (a/c))] + 14 [1 - (a/c)]^{24} \text{ and } g = 1 + [0.1 + 0.35(a/t)^2] (1 - \sin \phi)^2$$

$$f = [(a/c)^2 \cos^2 \phi + \sin^2 \phi]^{1/4} \text{ and } k = [\sec\{\pi a / 2b\} \sqrt{a/t}]^{1/2}$$

As seen Table 1 differences are found when values for the shape factor are read from the data tabulated in [1i] as opposed to evaluated from these equations. For all a/c with a/t small (e.g. 0.2) the differences are small but increase up to 12% for the larger a/t values at all a/c , the equations giving a result that is larger than the tabulated values.

An earlier comparison of all known results drawn from fourteen references was given in [9]. For shallow surface cracks, i.e. $a/t < 0.3$, there was close agreement, i.e. about 5%, between all fourteen cases regardless of the crack ellipticity. Results for deeper cracks, however, showed considerable differences, as much as 80%. One example from [9] is shown Fig.1. When correlated with experimental data from brittle epoxy material, results from Raju and Newman [10] showed the best fit.

2. SEMI-ELLIPTICAL SURFACE CRACKS IN THIN SHELLS

Only circumferential cracks are considered here. Most published data are for axial defects subjected to internal pressure. These include [13] using BIE. Reference [14] compared its own FE results at the apex, $\phi = \pi/2$, with those of Refs. [12] & [13] and showed less than 8% differences for any value of a/t or a/c . At the free surface, results from [12] were lower than those from the other two (which continued to agree with each other) by as much as 40% for the deep crack, i.e. $a/t = 0.8$. In [15] empirical equations fitted to FE results for the shape factor for a wide range of crack shapes were given. Comparison of [15] with [12] and [14] showed differences of only 2% with BIE and 8% with FE. These equations are the same as for the plate case, above, with $\sigma = pR/t$ where R is radius, except

that for the cylinder

$$k = \left\{ \frac{R_o^2 + R_i^2}{R_o^2 - R_i^2} \right\} + 1 - 0.5 \sqrt{a/t} \quad (a/t)$$

where R with subscripts 'o' or 'i' is the outer or inner radius respectively. Circumferential semi-elliptical surface cracks were considered by Delale and Erdogan [16], Ezzat and Erdogan [4], and Raju and Newman [3]. Refs [4] and [16] used a line spring model and [3] a 3D FE method. In [16] axial cracks were also considered and results were found which were some 10% higher than those reported by [15]. This makes the results from the line spring model some 18% higher than those in [14]. This comparison may serve as a guide for the circumferential defect where a direct comparison between the line spring model, FE, and BIE cannot be made based on present data. The 3D FE computations of [3] gave results 10% lower than those of [16] for a very deep circumferential crack, $a/t = 0.8$, with $a/c = 0.775$. Comparison for depths of other shapes is difficult. The computations [3] actually cover a very limited range of crack shapes, particularly in the a/c sense. Besides the semi-circular, only two other rather small ellipticities of $a/c = 0.8$ and 0.6 were computed.

B. PRESENT NUMERICAL COMPUTATIONS

1. GENERAL DESCRIPTION OF THE METHOD

The basics of the BIE method used are well documented, e.g. see Refs. [17 and 18], and will not be presented here. The BIE method has been widely applied to 3D crack problems since it is generally less expensive to use than FE, one case has already been described, [13]. The program used for the present computations was applied earlier to thick cylindrical vessels, [19]. To evaluate the stress intensity factor several methods are available. The first two use crack face displacements, q , evaluated for points on the crack face along a line normal to the crack front

$$q = (4K/E) \sqrt{r/2\pi} \quad \text{and hence } K = [(E/4) \sqrt{2\pi}] (q/\sqrt{r})$$

where r is the distance from the crack tip and E is the elastic modulus. In Method i direct extrapolation to $r = 0.0$ gives the magnitude of K . Method ii involves the plot of q versus the square root of r . This gives a straight line passing through the origin, the slope of which gives K . This latter method is generally considered to be more accurate since it does not rely on difficult extrapolation near $r = 0.0$. Other methods include of course extrapolation of stresses or strains in the body rather than of crack face displacements, change of crack area to find the energy release rate, contour integral evaluation or use of elements with nodes displaced to introduce a half power singularity. The last two, though used elsewhere in BIE studies, are not available on the present program but it is hoped to examine them later.

2. PLATE CASES STUDIED

Four cracked plate (P) geometries were computed in tension (t), D with uniform end displacement, and S with uniform end stress. W is plate width and h is plate height. In each case a symmetric quarter of the plate was modelled.

Case Pt0D, Pt1D and Pt1S	$a/c = 0.333$	$a/t = 0.5$	$W/t = 12.8$	$h/c = 25.6$
Case Pt2D	0.4	0.4	19.2	38.4
Case Pt3D and Pt3S	0.4	0.4	5.0	5.0
Case Pt4D and Pt4S	0.4	0.2	10.0	10.0

All meshes other than for Case 0 used a mesh with points on the edge of the crack face lying on a line normal to the crack front. Comparison of the result for 0D and 1D showed an increase of 1.5% for 1D and all subsequent meshes used that form. For Cases 0D and 1S a comparison was made of methods i and ii for finding K. The latter results were 4% higher and later results using method i were increased by that amount. In Cases S uniform stress rather than uniform end displacement was applied affecting K by +1.6% for Case1S, - 0.5% for Case3S and no effect for 4S. The other parametric ratios of width and length to crack size in Case 1 are not common within the existing data so other cases with geometry nearly identical to the published data were computed. Cases 2 and 3 show a difference of only 2% for the change in W/c and h/c.

As seen in the tabulated data, Table2, the agreement with the results of [2], not now usually thought to be the best, is good for Cases 1D or S, quite close (e.g.5%) for Cases 2 and 3 but less close (e.g.10%) for the shallow crack, Case 4 . A finer mesh Case 4D and S for a shallower crack, $a/c = 0.4$, $a/t = 0.2$, was also computed but again gave results 11% below [2]. Comparison with what are commonly taken to be the most reliable results, [1], is at the 15% (low) level throughout. All cases are shown Fig.2 in relation to the tabulated data of [1i].

It is not possible to resolve the differences of up to 18% between the present data and those of [1] or [10] from the few cases yet studied. In so far as even greater differences are already quoted in the literature, see [9] and Fig. 1, doubt on the correct value must exist. It is noted that the comparison in [9] is between several methods of analysis, the line spring model, various versions of the alternating method, and FE computations. The FE computations were obtained essentially from one source, and hence comparisons with other FE (or BIE) computations were not made. Such comparisons of different FE and a BIE method were referred to above for axial cracks in shells, [12-15], and differences of up to 8% for two sets of FE computations were noted, albeit differing in the one case by only 2% from the BIE result of [13]. The present few results are not seem strong enough to seriously challenge existing cracked

plate data particularly as the present results are low even for the shallow crack ($a/t = 0.2$) where the other data are coming together. The lack of agreement implies further BIE and perhaps FE analysis is required, be it by this program using different meshes and other refinements or a different program, before the differences can be resolved.

3.CIRCUMFERENTIAL CRACKS IN SHELLS

i) Some computed BIE results and comparisons at the apex.

Three configurations have been computed for cylinders with circumferential cracks (Cc) on the outer face with applied tension (t) loads and for Case 2, in local bending.

Only a quarter of the body was modelled, strictly implying two symmetric cracks.

Case Cct1	$a/c = 0.14,$	$a/t = 0.5,$	$R/t = 29.1,$	$h/c = 26.1,$
Case Cct2 and 2B	0.6	0.5	11.0	19.3
Case Cct3	0.6	0.6	11.0	16.0

As seen Table 3, the result of 1.63 (inferred for method ii) for Case Cct1 compares favourably with the value 1.637 from the line spring model of [4]. To compare with 3D FE results, the data of [3] would have to be extrapolated grossly. Two further cases, Cct2 and Cct3 were computed, with geometric details identical to two in [3]. Results in Table 3, show agreement with the 3D FE

work of [3] to about 5%. For Case 2B a mesh more uniform remote from the crack was used but the result differs only slightly. The results are some 12+or-4% below the line spring data of [4] which might generally be regarded (though not demonstrated) to be less accurate than the FE data. It is noted that the present values increase from $a/t = 0.5$ to 0.6 less rapidly than do either of the existing values. This must raise doubts whether the good agreement of 5% found with [3] (and indeed other 'spot' agreements reported in the literature at that level) is genuine or fortuitous. To resolve that a wider range of cases must be studied, although as seen for Case 1, the range of existing data is restricted so that extensive results would by their nature, have to be taken on trust.

ii. Variation of Y around the crack front.

For Case Cct1 the shape factor Y was examined around the crack front using method i. It gradually decreased from 1.57 at the apex to about 0.6 at 36° to the major axis of the ellipse, Fig.3. This trend is similar to the results of Kobayashi et al [12] whereas in [13] and [14] both tend to give an increasing value for the shape factor at positions away from the apex. In [15] complete axially symmetric cases with internal pressure were studied so that variation around the crack front did not occur. However, for axial cracks an increasing trend was noted with little difference in the shape factor for inner or outer wall defects. Ezzat and Erdogan [4] evaluated the shape factor at the apex only, implying either that that is the most severe case or that K does not vary along the crack front. A more complex picture emerged from the 3D FE computations of [3];

1. The shape factor at both the apex and surface increase with increasing a/t for any a/c . The increase of the former appears linear whilst the latter is parabolic.
2. At any given crack depth ratio, a/t , the value of F at the apex decreases as a/c increases; for the same a/t , the shape factor at the surface behaves in completely the opposite way, i.e. F increases with a/c .

iii. Local wall bending.

Crack Cc2 was also computed when subjected to local wall bending, Ccw2B. This bending case was more sensitive to mesh pattern remote from the crack than were the tension cases. It is not the case examined in [20] where the whole cylinder is bent. Here, the uncracked body remains axially symmetric and the applied stress dies away as an exponentially damped wave according to classical shell theory. It is a first step towards cases of local wall bending in the nodal joints of offshore structures. The result is appended to Table 3, the Y value at the apex being some 20% less than the tensile case. The value at the surface is higher than at the apex. The nominal applied stress used in evaluating Y is the stress in the shell at the position of the subsequent crack. It follows from shell theory that a value of K would depend on the distance of the crack from the loaded end.

CONCLUSION

- 1) A comparative analysis of shape factor data for semi-elliptical surface cracks in both flat plate and cylindrical shell geometries from the open literature reveals considerable disagreement. The FE results for plates are larger than the main other data from the line spring method, whereas for shells, the FE results are smaller. The present rather few BIE cases fall within the global spread in both cases.
- 2) For plates, the present BIE results are in better agreement with the line spring results of Shah and Kobayashi [11] than those of Raju and Newman [1,9,10],

which are usually taken to be the most reliable. It is not possible with the present few data to account for the difference and hence be certain which results are in fact most accurate.

3) For circumferential cracks in a cylindrical shell, the present results using BIE method fall below results from the line spring model [4] but close to those from 3D FE computations [3], i.e. the reverse of the plate case.

4) A single case of local wall bending of a circumferential crack in a cylinder suggests the use of tensile data will be conservative at the apex, in this case by 20%.

ACKNOWLEDGEMENTS

The present BIE computations, funded under an SERC Marine Technology Programme, were performed by Mr C.E.Noah, Computer Programmer.

REFERENCES

1. & 1i J.C.Newman Jr. and I.S. Raju, ASTM STP 791, 1983, pp. I238-265 (see also Newman NASA with the actual data)
2. D.P.Rooke and D.J.Cartwright, HMSO, London 1976.
3. I.S.Raju and J.C.Newman Jr., ASTM STP 905,1986,pp.323-330
4. H.Ezzat and F.Erdogan, J.Pres.Ves.,TRANS ASME,1982,Vol 104, pp.789-805.
5. C.B.Buchalet and W.H. Bamford, ASTM STP 590, 1976, pp.385-402.
6. R.Labbens et al ,ASTM STP 590, 1976, pp.368-384.
7. O.L.Bowie and C.E. Freese, Eng.Fract. Mech., Vol 4, 1972, pp.315-321.
8. V.Kumar et al , ASTM STP 803, 1983, pp.I306-353.
9. J.C.Newman Jr. ,ASTM STP 687,1979,pp.16-42.
10. I.S.Raju and J.C.Newman.Eng.Fract.Mech., Vol 11, No4, 1979, pp. 817-829.
11. R.C.Shah and A.S.Kobayashi,'The surface crack physical problem and computational methods'. ASME, New York, 1972.
12. A.S.Kobayashi et al, J of Pres. Vess. Tech., TRANS ASME, 1977, pp.83-89.
13. J.Heliot et al, ASTM STP 677, 1979, pp.341-364.
14. J.J.McGowan and M.Raymond, ASTM STP 677, 1979, pp. 365-380.
15. J.C.Newman and I.S.Raju, J of Pres. Vess. Tech. ,TRANS ASME, 1980, pp.342-346. Also 1982, Vol 104, pp.293-298.
16. F.Delale and F.Erdogan, J of App. Mech.,1982, Vol 49, pp.97-102. Also J. of Pres. Vess. Tech., TRANS ASME, 1981, Vol 103, p160.
- 17.F.J.Rizzo, Quart.Appl. Maths., 1976, Vol 25, pp.83-95.
- 18.J.C.Lachat and J.O.Watson, Int.J.Num.Meths.Eng.,1976,Vol 10, pp.991-1005.
- 19.H.Navid et al ,Int.J.Pres.Ves.&Piping, Vol 18, No 4, 1985, pp.241-255.
- 20.I.S.Raju & J.C.Newman. ASTM STP 905, 1986, pp.789-805.

Table 1
Comparison of 3D FE values for Y with the approximations from [1] : Data for apex for surface semi-elliptical cracks subject to tensile loading

a/c	a/t=0.2		a/t=0.4		a/t=0.6		a/t=0.8	
	FE	Eqn (%)*	FE	Eqn (%)*	FE	Eqn (%)*	FE	Eqn (%)*
0.2	1.117-1.133	(1.4)	1.294-1.335	(3.1)	1.563-1.633	(4.3)	1.762-1.972	(10.6)
0.4	0.989-0.933	(-0.4)	1.065-1.103	(3.5)	1.191-1.258	(5.3)	1.257-1.421	(11.5)
0.6	0.869-0.869	(0.0)	0.897-0.935	(4.1)	0.963-1.028	(6.3)	0.990-1.126	(12.1)

* % difference in the values from the equations in [1] and tabulated FE results in [1i].

TABLE 2
RESULTS FROM SEMI-ELLIPTICAL SURFACE CRACKS IN PLATES SUBJECT TO TENSILE LOADING; Data for apex

Crack Case	No. of Elements	LEFM SHAPE FACTOR Y at APEX ⁺			
		1	2	3 and (% from 2)	4 and (% from 2)
Pt0D*	153	0.993	1.03	1.04 (0.9)	1.26 (18.3)
Pt1D	157	1.008	1.05	1.04 (-0.9)	1.26 (16.7)
Pt1S*	157	1.024	1.07	1.04 (-2.8)	1.26 (15.1)
Pt2D	157	0.877	0.91	0.97 (6.2)	1.065 (14.6)
Pt3D	75	0.891	0.93	0.97 (4.3)	1.065 (12.7)
Pt3S	75	0.884	0.92	0.97 (5.2)	1.065 (13.6)
Pt4D	121	0.8049	0.837	0.94 (11.0)	0.989 (15.4)
Pt4S*	121	0.8046	0.837	0.94 (11.0)	0.989 (15.4)

+ Col 1 present work using method i, Col 2 elevated 4% from 1 (* actually evaluated method ii). Col 3 from Ref 2, Col 4 from Ref 1 (these gave best comparison with experimental data)

TABLE 3
RESULTS FROM CIRCUMFERENTIALLY CRACKED CYLINDERS SUBJECT TO TENSILE STRESS ; Data for apex

Crack Case	No. of Elements	LEFM SHAPE FACTOR Y ⁺			
		1	2	3 and (% from 2)	4 and (% from 2)
Cct1	157	1.57	1.634	1.637 (0.02)	(---)
Cct2	113	0.831	0.864	1.033 (16.0)	0.912 (5.2)
Cct2B	121	0.827	0.860	1.033 (16.1)	0.912 (5.7)
Cct3	11	0.876	0.911	0.995 (8.4)	0.938 (2.9)

+Col 1 present work using method i, Col 2 elevated by 4% from Col 1 Col 3 from Ref 4, Col 4 from Ref 3.

LOCAL WALL BENDING CASE. i) apex, ii) surface

Ccw2B	121	i) 0.625	ii) 0.746	no other data known
-------	-----	----------	-----------	---------------------

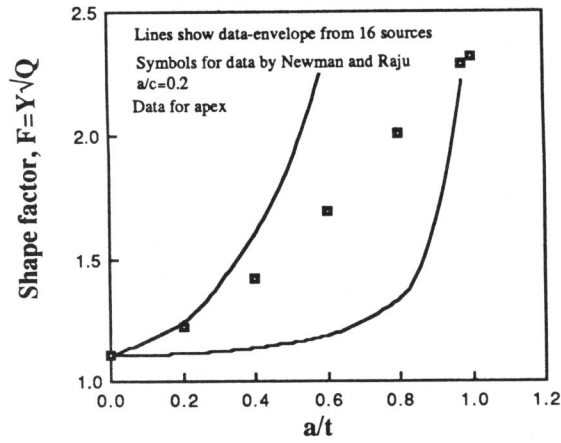


Fig.1 Data from Ref.1

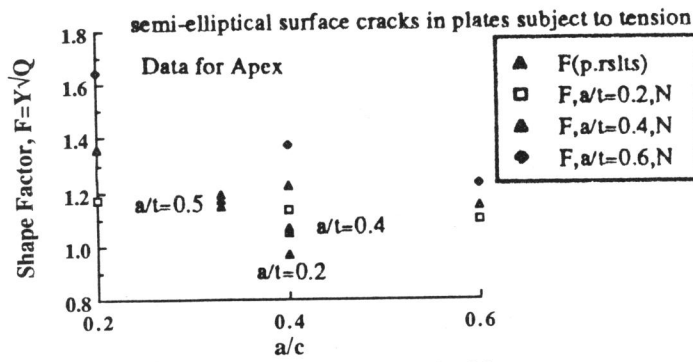


Fig.2 Comparison of present data and Ref 1

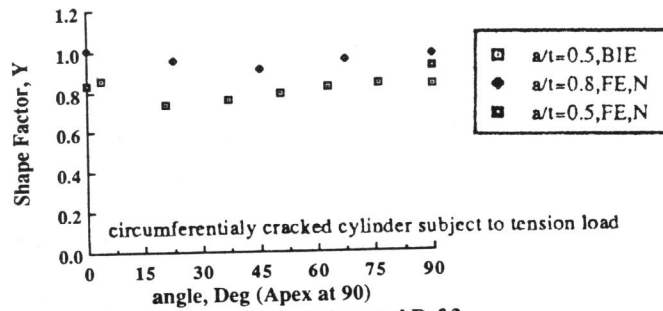


Fig. 3 Comparison of present data and Ref 3